Adsorption of Reactive Blue 19 onto Activated Carbon Prepared from Pomegranate Residual by Phosphoric Acid Activation: Kinetic, Isotherm and Thermodynamic Studies

E. Radaei[1], M. R. Alavi Moghaddam[*2] and M. Arami[3]

[1.] M. Sc., Department of Civil and Environmental Engineering, Amirkabir University of Technology, P. O. Box: 15875-4413, Tehran, Iran.

[2.] Associate Professor, Department of Civil and Environmental Engineering, Amirkabir University of Technology, P. O. Box: 15875-4413, Tehran, Iran.

[3.] Professor, Department of Textile Engineering, Amirkabir University of Technology, P. O. Box: 15875-4413, Tehran, Iran.

ABSTRACT

In this study, the adsorption of Reactive blue 19 onto pomegranate residual-based activated carbon was investigated in aqueous solution. The activated carbon prepared by phosphoric acid activation under air condition. PRAC was characterized for its surface chemistry by point of zero charge measurements, Scanning Electron Microscopy and nitrogen adsorption at 77 K. The effect of operational parameters including contact time, initial pH, adsorbent dose, initial dye concentration and particle size were studied. Results showed that an optimum dye removal efficiency (96.7%) was observed at initial pH=11, contact time of 5 min, adsorbent dose of 3.25 g/L, initial dye concentration of 200 mg/L, and particle size of 63-149μm. The adsorption process was found to follow the Temkin isotherm equation (R^2=0.975) and second-order kinetic model (R^2=0.999). Furthermore, thermodynamic parameters such as ΔG°, ΔH°, and ΔS° were calculated. Prog. Color Colorants Coat. 7(2014), 245-257 © Institute for Color Science and Technology.

1. Introduction

Dyes are water-soluble and intensely colored substances used for the coloration of various substrates, including paper, leather, hair, food, and textiles [1]. About 10-15% of these dyes are released in effluents during dyeing processes [2]. Color removal from industry or domestic effluents has drawn considerable attention in the last few years because of its toxicity and visibility.

Adsorption process has been found to be a prominent method of treating aqueous effluent in industrial processes for a variety of separation and purification purpose [3]. For color removal, this

*Corresponding author: Alavi@aut.ac.ir

technique also found to be highly efficient in terms of initial cost, simplicity of design, ease of operation and insensitivity to toxic substances [4]. Adsorption using activated carbon, due to its high specific surface area and adequate pore size distribution, is currently of great interest for removal of different types of dyes and pigments. A wide range of raw lignocellulosic materials such as coal, peat, wood and various agricultural by-products have been utilized for the preparation of activated carbon [5]. Pomegranate is an important fruit crop of many tropical and subtropical regions of the world, grown especially in the moderate climates of Mediterranean countries like Iran. It is widely consumed fresh and in processed forms as juice and jams. Pomegranate residual is a by-product of the pomegranate juice factory. Several studies have been conducted on preparing activated carbon from pomegranate peel or seed [6-9]. However, to the best of our knowledge, there is no research about activated carbon prepared from pomegranate residual (include seed and peel) via activation by phosphoric acid at 500 °C. Phosphoric acid was chosen as it has become a widely accepted chemical activator as an alternative to zinc chloride due to environmental concerns and its easily recovery [10].

The main aim of the present study is investigation of the application activated carbon for removal of Reactive Blue 19 from aqueous solution. The activated carbon is prepared from pomegranate residual by chemical activation with minimum phosphoric acid (25 wt.%) at lowest temperature (1 hr at 500 °C). For this purpose, the effect of different parameters such as contact time, initial pH, adsorbent dose, initial dye concentration and particle size was surveyed in addition to characterize the prepared activated carbon. Isotherm, kinetic, and thermodynamic of adsorption process was also studied.

2. Experimental

2. 1. Preparation and characterization of activated carbon

In this study, pomegranate residual was collected from Meykhosh juice industry in Yazd/Iran. Pomegranate residual was dried in an oven for 2 h at 100 °C until a constant weight was reached. It was ground in a ball mill, passed through No. 8 mesh sieve, and then collected for the subsequent examination. The powder was soaked in 25 wt% phosphoric acid (ratio of 1:1 w/v) at room temperature for 24 h. The sample is then decanted, dried in a muffle furnace under air condition for 1 h at 500 °C. Then the samples were washed sequentially several times with hot distilled water to reach neutral pH. Finally, pomegranate residual-based activated carbon (PRAC) powder was prepared and sieved into two particle sizes (PRAC1: 63-149μm (mesh 230-100) and PRAC2: 149-297μm (mesh 100-50).
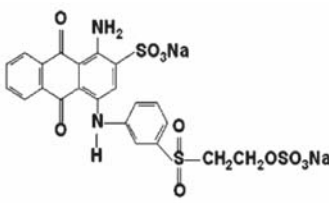
Scanning electron microscope (SEM) was used to characterize the morphology of the samples using a XL-C model SEM analyzer (Philips, Netherlands). The textural properties of adsorbents were also analyzed by N_2 adsorption/desorption isotherms at 77K using an Autosorb 1 analyzer (Quantachrome Corporation, USA). The specific surface area was calculated by Brunauer-Emmett-Teller (BET) method which is named S_{BET}. The FTIR spectrum of PRAC was achieved byPerkin-Elmer Spectrophotometer Spectrum One in the range of 400-4000 cm^{-1}. For the determination of point of zero charge (PZC) of PRAC, the instruction of Calvete et al. (2009) was used [11].
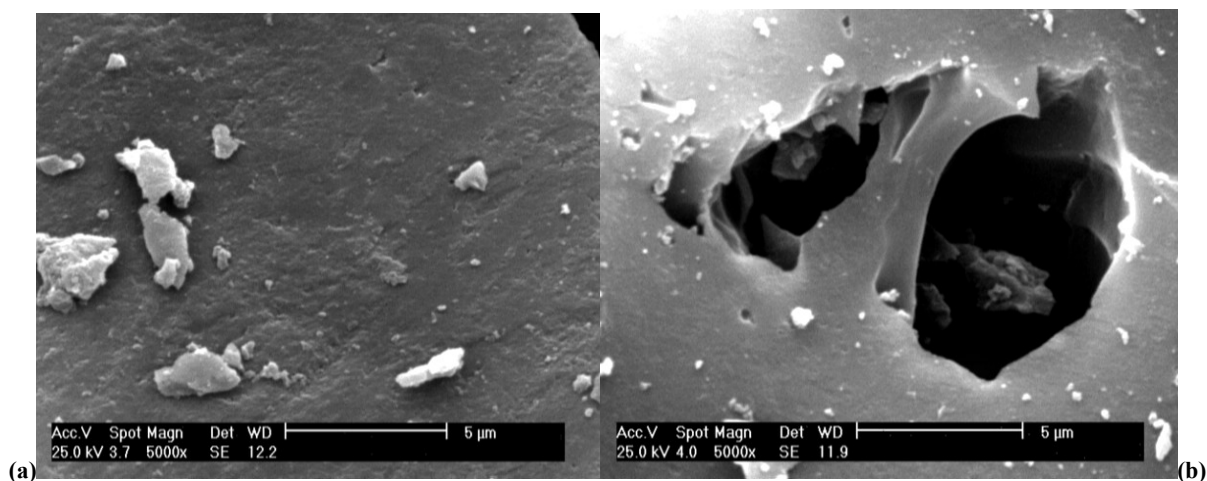
For this test, 0.05 M NaCl was prepared and its initial pH was adjusted between 2 and 12 using 1 M NaOH and HCl. Then, 50 ml of 0.05 M NaCl was poured in 250 ml beakers and 0.05 g of PRAC was added to each solution. These beakers were kept for 48 hours and the final pH of the solutions was measured with a pH meter.

2. 2. Preparation of dye-containing solutions and experimental procedure

Dye solution was prepared by dissolving Reactive blue 19 (RB19) which was provided by the Alvan Sabet Company. The chemical structure and characteristics of the selected dye is presented in Table 1. For the preparation of synthetic wastewater, a stock dye solution of 1000 mg/L was prepared in distilled water and then diluted to the range of 100 and 500 mg/L according to actual concentration of textile wastewater in Iran [12]. The solution pH measurement was carried out using a 340i/SET pH meter (WTW-Germany) and was adjusted by 1M hydrochloric acid or 1M sodium hydroxide. The dye solution and adsorbent was agitated by a jar test at 150 rpm at ambient temperature. A six beaker jar test apparatus from Zag-Chemi Company in Iran was used to simulate the adsorption process.

Table 1: Chemical structure and properties of RB19.

Characteristics	Values	Chemical structure
Molecular formula	$C_{22}H_{16}N_2Na_2O_{11}S_3$	
λ_{max} (nm)	594	
Molecular weight (MW)	626.54	

Figure 1: SEM images of used PRAC sample (a) before and (b) after adsorption process.

All samples were filtered through glass fibre filters GF/A (pore size: 4 μm). The clear supernatants were analyzed for RB19 dye concentrations using a UV-vis HACH spectrophotometer (DR/4000).

Percentage of dye removal was calculated by equation (1).

$$\text{Dye removal (\%)} = \frac{C_0 - C_t}{C_0} \times 100 \qquad (1)$$

where C_0 and C_t (mg/L) are the initial dye concentration and concentration at time t (min), respectively.

3. Results and discussion

3. 1. Characterization of PRAC

SEM images (Figure 1) show the morphology of PRAC samples before and after the adsorption process. From Figure 1 it is clear that PRAC has numerous pores which are the accessible sorption sites for dye

uptake. The results of the BET method showed that the average S_{BET} of PRAC was 425.50 m^2g^{-1}, which is higher than earlier pomegranate activated carbon [7]. Typical values of BET for commercial activated carbons were usually between 400 and 1500 m^2g^{-1} [13].

FTIR spectra of the PRAC samples before and after activation and adsorption are shown in Figure 2. In the FTIR spectra of PRAC before activation, the band at 3395.46 cm^{-1} is due to O-H and N-H stretching. While the bands at 2926.91 and 1729.10 cm^{-1} reflect C-H stretching and C=O, respectively. The bands at 1613.51 and 1230.39 cm^{-1} correspond to N–H bending and phosphorous-containing group P=O stretching, respectively.

Figure 2 also shows the spectra before and after adsorption. In the FTIR spectra of PRAC before adsorption, the band at 3432.43 cm^{-1} is due to O-H and N-H stretching, while the bands at 2922.73 and 2851.89 cm^{-1} reflect C-H stretching. The bands at

1616.71 and 1204.81cm^{-1} correspond to N-H bending and phosphorous-containing group P=O stretching, respectively.

The intensity of all peaks clearly decreased after the RB 19 adsorption, indicating that O-H, N-H, C-H, and phosphorous-containing group were involved in the RB 19 adsorption. The peak positions at 3432.43, 2922.73, 2851.89, 1616.71, and 1204.81 cm^{-1} before adsorption shifted to 3432.03, 2923.72, 2852.7, 1614.25, and 1230.35 cm^{-1} after adsorption, respectively.

The final pH values were plotted against the initial pH in Figure 3. The pH$_{pzc}$ is the point where the curve corresponding to Final pH versus Initial pH crosses the line in which the initial pH = final pH.

As shown in Figure 3, pH$_{PZC}$ of PRAC is considered equal to 2.43. The surface charge of PRAC is neutral at pH$_{PZC}$ below which the adsorbent surface is positively charged. Above the pH$_{PZC}$, the adsorbent surface is negatively charged [14]. Points of zero charges (pH$_{PZC}$) of the activated carbons produced from pomegranate seeds were found to be in the range of 7.35 and 9.41 [9].
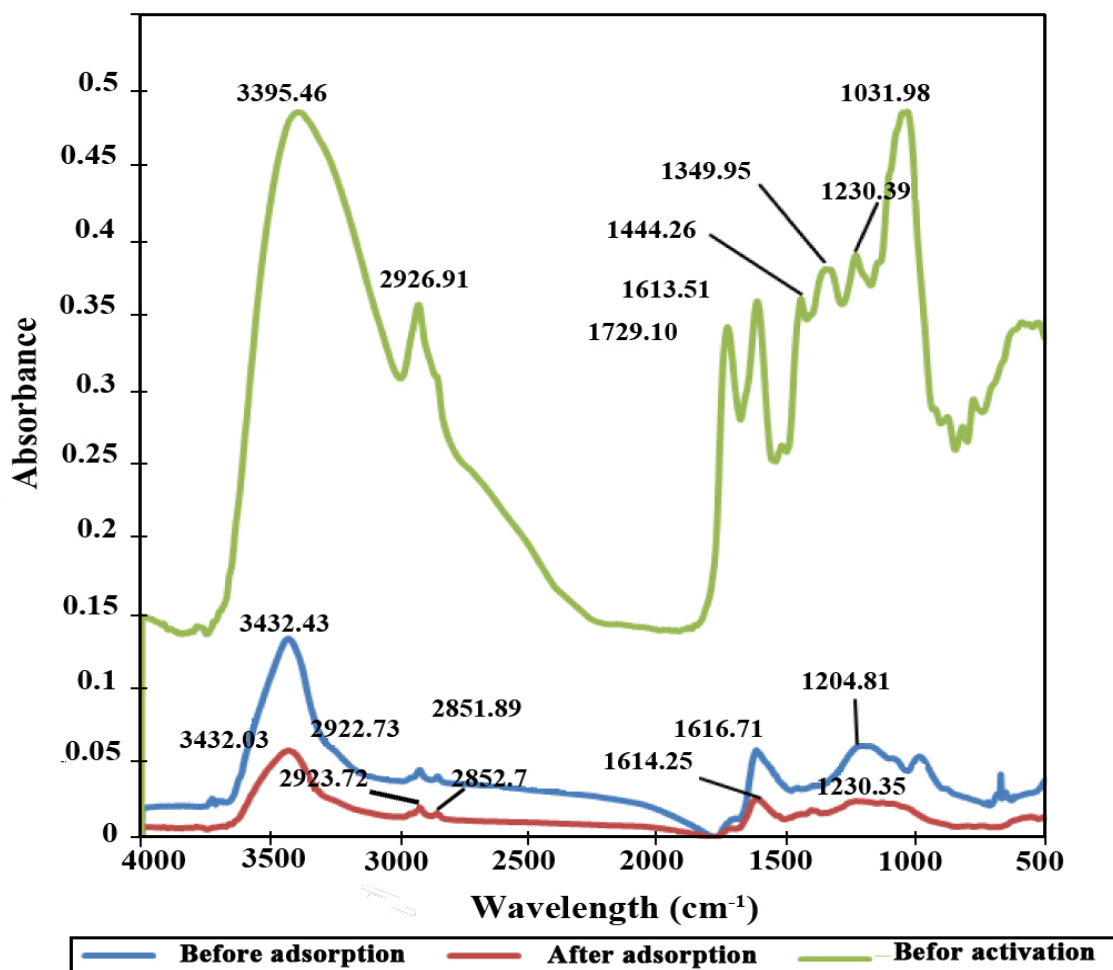

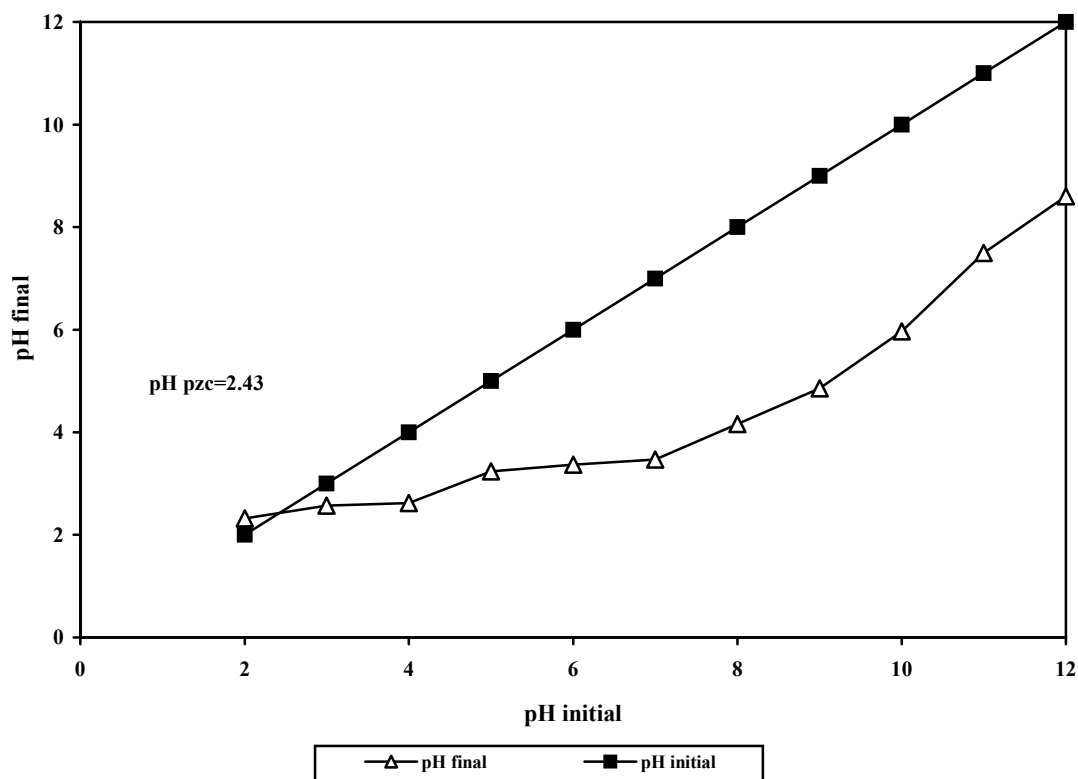**Figure 2:** The FTIR spectra of samples before and after activation and adsorption.

Figure 3: Point of zero charge for PRAC.

3. 2. Influencing factors

3. 2. 1. Effect of contact time

The effect of contact time on RB19 adsorption efficiency and adsorption capacity is presented in Figure 4. The experiments of this step were done in the conditions of constant initial concentration of 200 mg/L, PRAC dose of 3.25 g/L, and pH 11. The adsorption efficiency and the adsorption capacity increased with agitation time. The initial rate of dye uptake was fast, so that the equilibrium was reached rapidly.

This may be due to the fact that the structure of PRAC has much higher micro- and macro-porosities. Similar results have been reported in literature on the extent of removal of dyes [13, 14]. It was shown that 89.16% and 96.65% removal of RB19 occurred after 1 and 5 minutes, respectively. In addition, after 5 minutes no significant changes were observed. Moreover, as shown in Figure 4, dye adsorption decreased as the particle size was increased, hence, the percentage of the removed dye was also decreased.

3. 2. 2. Effect of initial pH

The effect of initial pH was studied by performing the adsorption experiments at different pH levels, i.e. 3.0, 5.0, 7.0, 9.0 and 11.0. According to pH_{PZC} value, PRAC surface is negatively charged (pH> pH_{PZC}). As shown in Figure 5, pH 11 had higher removal efficiency, whereas, less efficient results were achieved by pH 7.

At neutral pH, there is a possibility of oxidation of the surface oxygen complexes, which may impart positive charge to the activated carbon surface [16]. Similar results have been reported in literature on the extent of removal of dyes [17-19]. Figure 5 shows the same behaviour of PRAC1 and PRAC2 as a function of pH. However, PRAC2 dye removal efficiency is less than PRAC1 under same conditions.
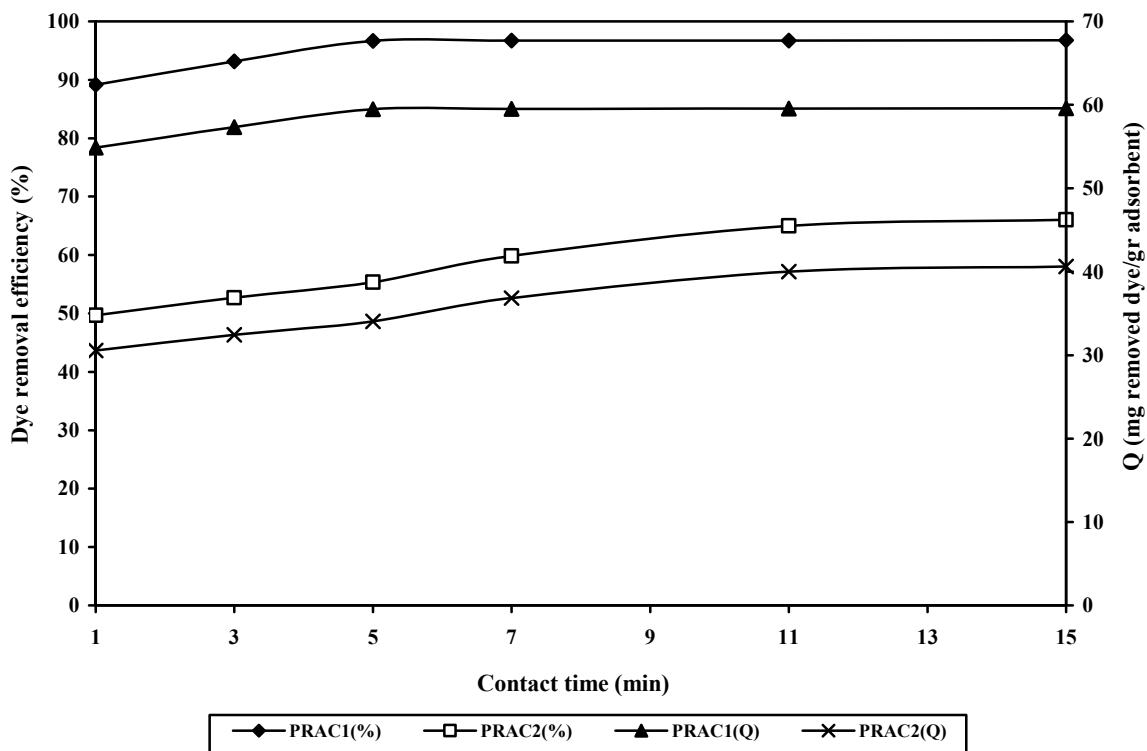
Figure 4: Effect of contact time on RB19 removal efficiency (initial pH=11, adsorbent dose =3.25 g/L, and initial dye concentration=200 mg/L).
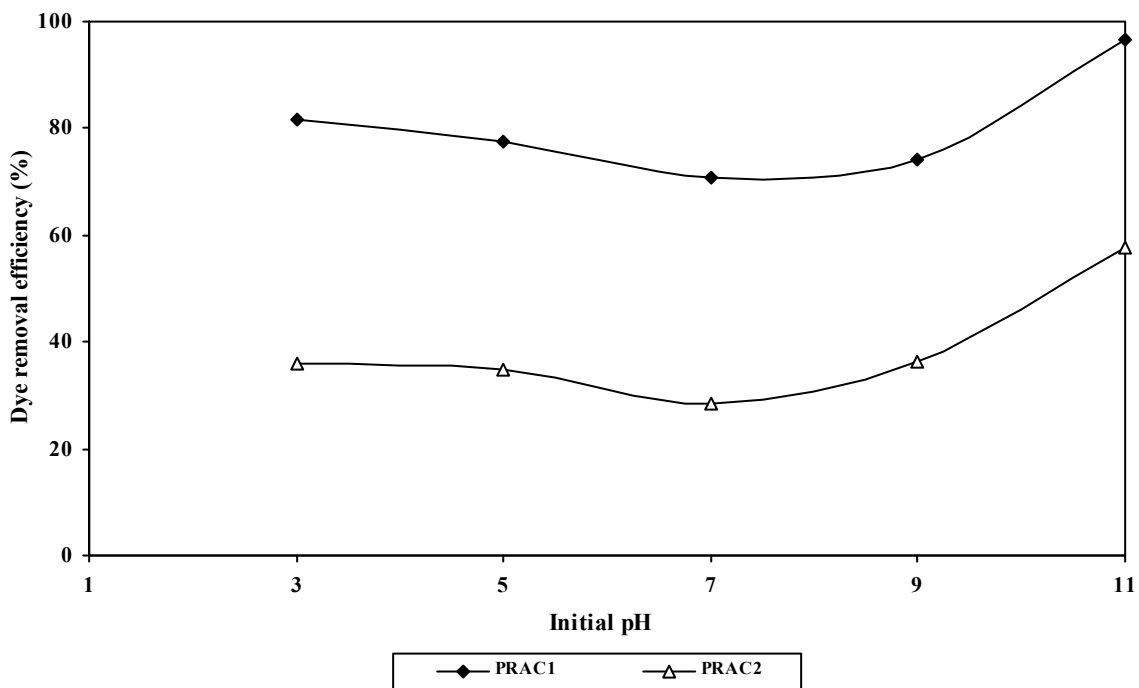

Figure 5: Effect of initial pH on RB19 removal efficiency (contact time=5 min, adsorbent dose=3.25 g/L, and initial dye concentration=200 mg/L).

3. 2. 3. Effect of adsorbent dosage

Adsorbent dosage is an important parameter for the adsorption process because this determines the capacity of an adsorbent for a given initial concentration of the adsorbate. The effect of PRAC dose on the adsorption of RB19 dye is presented in Figure 6.
The result shows that the adsorption of RB19 dye increases up to a certain limit and then it remains constant.

An increase in adsorption with adsorbent dosage can be attributed to the increased surface area and the availability of more adsorption sites. Similar results have been reported in previous studies [12, 20]. Furthermore, as shown in Figure 6, for a given adsorbent dose, the dye adsorption decreased as the particle size increased.

3. 2. 4. Effect of initial dye concentration

Figure 7 shows the effect of RB19 dye concentration on the dye uptake. The adsorption percentage was found to decrease with increasing initial dye concentration. But the amount of adsorbate per unit mass of the adsorbent (Q) increased considerably so that the maximum amounts of Q were 104.3 and 59.6 mg/g for PRAC1 and PRAC2, respectively.

This may be due to the saturation of surface area and active sites of the adsorbent. Similar results were reported by Kannan and Sundaram (2001) for methylene blue adsorption on various activated carbons and Amin (2008) for reactive dye adsorption on sugarcane bagasse pith activated carbon [14, 21].

In Table 2 the maximum adsorption capacity of PRAC is compared with previous reported adsorbents for RB19 dye removal. As can be seen from Table 2, PRAC has high adsorption capacity of RB 19 from aqueous solution.

As shown in Figure 7, when the particle size decreased from 149 μm to 63 μm, the adsorption increased from 59.6 to 104.3 mg/g. The results suggest that the dye molecules do not completely penetrate into the particle. For larger particles, the diffusion resistance to mass transfer was great and the majority of the internal surface of the particle may not have been used for adsorption. Thus, the amount of adsorbed dye was minimal. Dye molecules preferentially adsorbed near the outer surface of the particle. The similar result was observed in previous studies [25, 26].

Table 2: Comparison of different adsorbents for the removal of RB19.

| Adsorbents	Using form	Adsorption capacity (mg/g)	References
Wood waste	Natural	30.92	[12]
Dried pulp and paper sludge	Natural	33.11	[22]
Pulp and paper sludge	Treated (with $ZnCl_2$)	47.7	[23]
Pulp and paper sludge	Acid treated (with H_2SO_4)	35.6	[23]
Pulp and paper sludge	Basic treated (with NaOH)	18.7	[23]
Basic oxygen furnace slag	Acid treated (with HCl)	60	[24]
PRAC	Activated carbon by H_3PO_4 activation	104.3	Present study
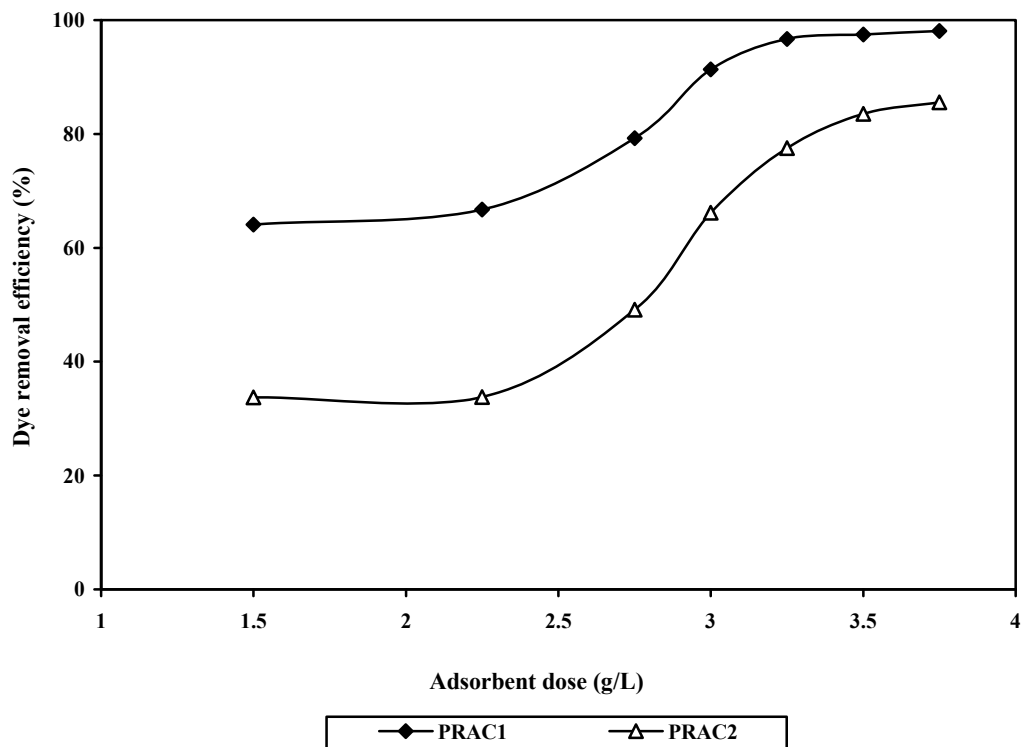
Figure 6: Effect of adsorbent dose on RB19 removal efficiency (contact time=5 min, initial pH=11, and initial dye concentration=200 mg/L).
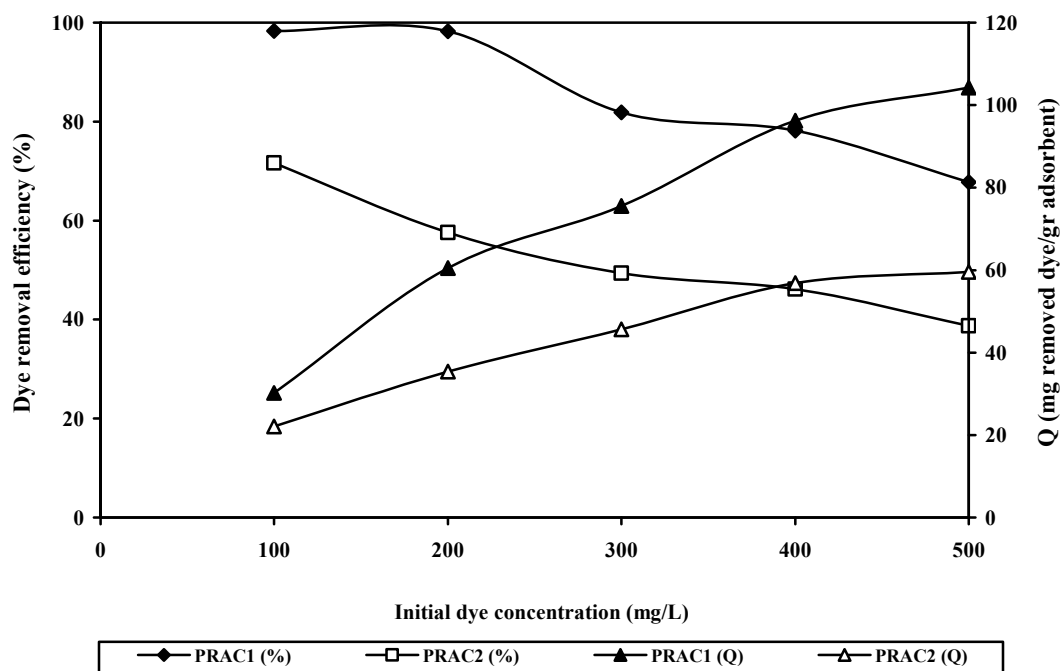

Figure 7: Effect of initial dye concentration on RB19 removal efficiency (contact time=5 min, initial pH=11, and adsorbent dose =3.25 g/L).

3. 3. Adsorption isotherms studies

To optimize the design of an adsorption system for the adsorption of adsorbates, it is important to establish the most appropriate correlation for the equilibrium curves. Langmuir, Freundlich, and Tempkin isotherm models were used to describe the non-linear equilibrium relationship between adsorption of the dye onto the activated carbon. Adsorption isotherm studies were carried out with different initial RB19 concentrations ranging from 150 to 500 mg/L, while the adsorbent dosage and pH were kept constant at 3.25 g/L and 11, respectively. The applicability of the isotherm models to the adsorption study was compared by judging the correlation coefficient (R^2) values.

3. 3. 1. Langmuir isotherm:

It is used to describe that uptake of dye molecules occurs on a completely homogenous surface by monolayer adsorption with negligible interaction between adsorbed molecules [6]. The Langmuir equation is presented in the linear form in equation (2):

$$\frac{1}{q_e} = \frac{1}{q_m} + \frac{1}{q_m b C_e} \qquad (2)$$

where q_e is the amount of adsorbate per amount of adsorbent at the equilibrium (mg/g), q_m is the maximum adsorption capacity (mg/g), b is adsorption equilibrium constant related to the free energy of adsorption (L/mg) and C_e is the equilibrium concentration (mg/L).

3. 3. 2. Freundlich isotherm:

It is derived by assuming a heterogeneous surface with a non-uniform distribution of heat of adsorption over the surface. The Freundlich equation is presented in the linear form in equation (3):

$$\ln q_e = \ln K_F + \frac{1}{n} \ln C_e \qquad (3)$$

where K_F is an indicator of the adsorption capacity (L/mg) and n is adsorption intensity.

3. 3. 3. Temkin isotherm:

This isotherm assumes that: (1) the heat of adsorption of all the molecules in the layer decreases linearly with coverage due to adsorbent/adsorbate interactions and (2) the adsorption is characterized by a uniform distribution of binding energies up to a maximum binding energy [27]. The Temkin isotherm equation is given in equation (4):

$$q_e = B_1 \ln K_T + B_1 \ln C_e \qquad (4)$$

where $B_1=RT/b$, T is the absolute temperature (K) , R (J/mol) is the universal gas constant and K_T is the equilibrium binding constant (L/mg).

Isotherm constants and correlation coefficient (R^2) are also presented in Table 3. The results illustrated that the Temkin adsorption isotherm was the best model (R^2=0.975) for dye adsorption on PRAC. This is in good agreement with FTIR results before and after adsorption. As was shown in FTIR analyzes, several chemical groups were involved in the RB19 adsorption

3. 4. Adsorption kinetics studies

Several models can be used to express the mechanism of solute adsorption onto an adsorbent. In order to develop a fast and effective model, investigations were made on adsorption rate. For the examination of the controlling mechanisms of the adsorption process (such as chemical reaction, diffusion control and mass transfer), several kinetics models are used to test the experimental data [28].

Table 3: Isotherm parameters' coefficients for RB19 dye adsorption onto PRAC.

Isotherm type	Isotherm constants	R^2
Langmuir	q_m=126.582, b=0.0528	0.929
Freundlich	KF=4.142 (L/mg), n=3.323	0.937
Temkin	K_T=1.042(L/mg), B_1=22.354	0.975

In this study, four kinetic models (the pseudo first-order, pseudo-second-order, Elovich, as well as intraparticle diffusion kinetic models) were used to fit the experimental data from the adsorption of RB19 dye onto PRAC at various pH values ranging from 3 to 11. For the pseudo-first-order model, a linear equation is obtained as follows:

$$\log(q_e - q_t) = \log q_e - \frac{k_1}{2.303} t \tag{5}$$

where q_e (mg/g) and q_t (mg/g) are the sorption capacities at equilibrium and time t, respectively, and k_1 (min⁻¹) is the rate constant. The pseudo-second-order model is presented by equation (6):

$$\frac{t}{q_t} = \frac{1}{k_2 q_e^2} + \frac{1}{q_e} t \tag{6}$$

Where k_2 is the pseudo-second-order rate constant of adsorption (g/mg. min). The simple Elovich model equation is expressed by equation (7):

$$q_1 = a + b \ln t \tag{7}$$

The slope and intercept of plot of q vs. $\ln(t)$ were used to calculate constants a and b. The intraparticle diffusion model is explored by using equation (8):

$$q_t = K_{dif} t^{0.5} + C^{`} \tag{8}$$

where C and K_{dif} (mg g⁻¹ min⁻⁰·⁵) are the intercept and the intraparticle diffusion rate constant, respectively.

Kinetics constants and correlation coefficient (R^2) for this study are presented in Table 4. Results demonstrated that the pseudo-second-order was the best model (R^2=0.999) for RB19 adsorption on PRAC. Furthermore, the calculated q_e value of pseudo second-order equation was compared with the experimental q_e value; the calculated q_e value is much close to the experimental q_e value (Table 5). Therefore, based on accuracy of model, the adsorption kinetics of RB19 was well described by pseudo second-order chemical reaction; this reaction was found significant in the rate-controlling step. As was shown in FT-IR analyzes before and after adsorption, several chemical groups were involved in the RB 19 adsorption. The mechanism of adsorption can also be described as chemisorptions, involving valence forces through sharing or the ion exchange of electrons between adsorbent and adsorbate as covalent forces.

Table 4: Adsorption kinetics constants.

pH	Pseudo-first-order		Pseudo-second-order		Elovich			Intraparticle diffusion		
	k_1 (min⁻¹)	R^2	k_2 (g/mg. min)	R^2	a	b	R^2	K_{dif} (mg g⁻¹ min⁻⁰·⁵)	C	R^2
3	0.196	0.996	0.0470	0.999	42.975	2.817	0.980	2.326	42.165	0.998
7	0.211	0.929	0.0708	0.999	25.859	1.970	0.978	1.605	25.348	0.969
9	0.241	0.969	0.0380	0.999	29.632	3.520	0.988	2.857	28.746	0.972
11	0.376	0.913	0.0234	0.999	39.299	5.280	0.976	4.355	37.804	0.984

Table 5: Adsorption kinetics constants (Pseudo-second-order).

pH	k_2 (g/mg. min)	R^2	$q_{e,exp}$	$q_{e,cal}$
3	0.0470	0.999	49.93	49.68
7	0.0708	0.999	30.63	30.51
9	0.0380	0.999	38.08	37.90
11	0.0234	0.999	51.94	51.93

Table 6: Thermodynamic parameters of the dye adsorption on PRAC.

Temperature (°C)	ΔG°(kJ/mol)	ΔH°(kJ/mol)	ΔS°(kJ/mol K)
25	-2.568		
35	-4.216	46.57	0.164
45	-5.865		
55	-7.513		

3. 5. Adsorption Thermodynamics

The thermodynamic parameters such as change in free (Gibbs) energy (ΔG°: kJ/mol), enthalpy (ΔH°: kJ/mol), and entropy (ΔS°: kJ/(mol.K)) were determined using the following equations [29]:

$$K_c = \frac{C_A}{C_S} \qquad (9)$$

$$LnK_c = (\frac{\Delta S^\circ}{R}) - (\frac{\Delta H^\circ}{RT}) \qquad (10)$$

$$\Delta G^\circ = \Delta H^\circ - T\Delta S^\circ \qquad (11)$$

where R (8.314 J/(mol.K)), T (K), C_A, C_S, and K_c (L/g) are the gas constant, the absolute temperature, the amount of dye adsorbed on the adsorbent of the solution at equilibrium (mol/L), the equilibrium concentration of the dye in the solution (mol/L), and the standard thermodynamic equilibrium constant, respectively. According to equation (10), ΔH° and ΔS° can be calculated from the slopes and intercepts of the plot of lnK_c versus 1/T, respectively.

Thermodynamic parameters were calculated by equation (9-11). Table 6 shows the negative values of ΔG° and positive ΔH°. Data indicate that the RB19 adsorption processes are endothermic reactions. The positive value of ΔS° suggests increased randomness at the solid/solution interface occurs in the internal structure of the adsorption of RB19 dye onto PRAC. The positive values of ΔH° indicate the presence of an energy barrier in the adsorption process and endothermic process [30].

The change in free energy for physisorption and chemisorption are between -20 and 0 kJ/mol and -80 to -400 kJ/mol, respectively [31]. The values of ΔG° in Table 6 are within the ranges of -20 and 0 kJ/mol,

indicating that the physisorption is the dominating mechanism.

4. Conclusion

In this study, pomegranate residual activated carbon (PRAC) has been prepared by the chemical activation of jute sticks using H_3PO_4 and used for removing RB19 from aqueous solution. The BET method showed that the average S_{BET} of PRAC was 425.50 m^2 g^{-1}. Furthermore, the determined point of zero charge was 2.43, which is considered as the pH_{PZC} of PRAC. Rapid adsorption was observed at initial contact time and then became constant after 5 minutes. The results indicated that the adsorbent particle size has an important influence on the maximum uptake, i.e. it increased from 59.6 to 104.3 mg/g when the particle size decreased from 149 μm to 63 μm.

The optimum dye removal efficiency (96.7%) was observed at initial pH 11, contact time of 5minutes, adsorbent dose of 3.25 g/L, initial dye concentration of 200 mg/L, and particle size of 63-149μm. Finally, isotherm studies revealed that the Temkin model (R^2=0.975) yields a somewhat better fit than the Langmuir and the Freundlich models. Kinetics studies also showed that the adsorption of the dye followed second-order kinetics (R^2=0.999). Thermodynamic studies indicated that the dye adsorption onto PRAC was a spontaneous, endothermic, and physical reaction.

guidance during the research.

5. References

1. M. Arulkumar, P. Sathishkumar, T. Palvannan, Optimization of Orange G dye adsorption by activated carbon of Thespesia populnea pods using response surface methodology, *J. Hazard. Mater.*, 186(2011), 827-834.

2. F. Bangash, A. Manaf, Thermodynamics of basic dyes (methylene blue and basic blue 3) adsorption on active charcoal prepared from the wood of ailanthus altisima, *J. Chem. Soc. Pak.*, 28(2011), 20-26.

3. Y. E. Benkli, M. F. Can, M. Turan, M. S. Celik, Modification of organo-zeolite surface for the removal of reactive azo dyes in fixed-bed reactors, *Water Res.*, 39(2005), 487-493.

4. V. K. Garg, M. Anita, R. Kumar, R. Gupta, Basic dye (methylene blue) removal from simulated wastewater by adsorption using Indian rose-wood sawdust: a timber industry waste, *Dyes Pigm.*, 63(2004), 243-250.

5. Z. Y. Zhong, Q. Yang, X. M. Li, K. Luo, Y. Liu, G. M. Zeng, Preparation of peanut hull-based activated carbon by microwave-induced phosphoric acid activation and its application in Remazol Brilliant Blue R adsorption, *Ind. Crops Prod.*, 37(2012), 178-185.

6. N. K. Amin, Removal of direct blue-106 dye from aqueous solution using new activated carbons developed from pomegranate peel: adsorption equilibrium and kinetics, *J. Hazard. Mater.*, 165(2009), 52-62.

7. M. Ghaedi, H. Tavallali, M. Sharifi, S. N. Kokhdan, A. Asghari, Preparation of low cost activated carbon from myrtus communis and pomegranate and their efficient application for removal of congo red from aqueous solution, *Spectrochim. Acta, Part A*, 86(2012), 107-114.

8. A. E. Nemr, Potential of pomegranate husk carbon for Cr(VI) removal from wastewater: kinetic and isotherm studies, *J. Hazard. Mater.*, 161(2009), 132-141.

9. S. Uçar, M. Erdem, T. Tay, S. Karagöz, Preparation and characterization of activated carbon produced from pomegranate seeds by $ZnCl_2$ activation, *Appl. Surf. Sci.*, 255(2009), 8890-8896.

10. M. Benadjemia, L. Millière, L. Reinert, N. Bender-douche, L. Duclaux, Preparation, characterization and methylene blue adsorption of phosphoric acid activated carbons from globe artichoke leaves, *Fuel Process. Technol.*, 92(2011), 1203-1212.

11. T. Calvete, E. C. Lima, N. F. Cardoso, S. L. P. Dias, F. a. Pavan, Application of carbon adsorbents prepared from the brazilian pine-fruit-shell for the removal of Procion Red MX 3B from aqueous solution-Kinetic, equilibrium, and thermodynamic studies, *Chem. Eng. J.*, 155(2009), 627-636.

12. A. Azizi, M. R. Alavi Moghaddam, M. Arami, Wood waste from mazandaran wood and the paper industry as a low cost adsorbent for removal of a reactive dye, *J. Residuals. Sci. Tech.*, 8(2011), 21-28.

13. A. R. Dinçer, Y. Güneş, N. Karakaya, E. Güneş, Comparison of activated carbon and bottom ash for removal of reactive dye from aqueous solution, *Bioresour. Technol.,* 98(2007), 834-839.

14. N. Kannan, M. M. Sundaram, Kinetics and mechanism of removal of methylene blue by adsorption on various carbons e a comparative study, *Dyes Pigm.*, 51(2001), 25-40.

15. A. Afkhami, R. Moosavi, Adsorptive removal of Congo red, a carcinogenic textile dye, from aqueous solutions by maghemite nanoparticles, *J. Hazard. Mater.*, 174(2010), 398-403.

16. S. V. Mohan, N. Chandrasekhar Rao, J. Karthikeyan, Adsorptive removal of direct azo dye from aqueous phase onto coal based sorbents: a kinetic and mechanistic study, *J. Hazard. Mater.*, 90(2002), 189-204.

17. A. Azizi, M. R. AlaviMoghaddam, M. Arami, Removal of a reactive dye using ash of pulp and paper sludge, *J. Residuals. Sci. Tech.*, 9(2012) 159–168.

18. P. Leechart, W. Nakbanpote, P. Thiravetyan, Application of waste wood-shaving bottom ash for adsorption of azo reactive dye, *J. Environ. Manage.*, 90(2009), 912-920.

19. I. D. Mall, V. C. Srivastava, N. K. Agarwal, I. M. Mishra, Removal of congo red from aqueous solution by bagasse fly ash and activated carbon: kinetic study and equilibrium isotherm analyses, *Chemosphere*, 61(2005), 492-501.

20. S. Sadri Moghaddam, M. R. Alavi Moghaddam, M. Arami, A Comparative study of Acid Red 119

dye adsorption onto dried sewage sludge and sewage sludge ash: isotherm, kinetic and desorption study, *J. Residuals. Sci. Tech.*, 7(2010), 199-207.

21. N. K. Amin, Removal of reactive dye from aqueous solutions by adsorption onto activated carbons prepared from sugarcane bagasse pith, *Desalination*,. 223(2008), 152-161.

22. A. Azizi, M. R. Alavi Moghaddam, M. Arami, Comparison of three treated pulp and paper sludges as adsorbents for RB19 dye removal, *J. Residuals. Sci. Tech.*, 8(2011), 117-124.

23. A. Azizi, M. R. AlaviMoghaddam, M. Arami, Performance of pulp and paper sludge for reactive blue 19 dye removal from aqueous solutions: isotherm and kinetic study, *J. Residuals. Sci. Tech.*, 7(2010), 173-170.

24. Y. Xue, H. Hou, Sh. Zhu, Adsorption removal of reactive dyes from aqueous solution by modified basic oxygen furnace slag: Isotherm and kinetic study, *Chem. Eng. J.*, 147(2009), 272-279.

25. O. Demirbaş, A. Karadağ, M. Alkan, M. Doğan, Removal of copper ions from aqueous solutions by hazelnut shell, *J. Hazard. Mater.*, 153(2008), 677-684.

26. X. Wu, K. N. Hui, K. S. Hui, S. K. Lee, W. Zhou, R. Chen, D. H. Hwang, Adsorption of basic yellow 87 from aqueous solution onto two different mesoporous adsorbents, *Chem. Eng. J.*, 180(2012), 91-98.

27. V. S. I. Mane, D. Mall, V. C. Srivastava, Use of bagasse fly ash as an adsorbent for the removal of brilliant green dye from aqueous solution, *Dyes Pigm.*, 73(2007), 269-278.

28. Y. S. Ho, Sorption studies of acid dye by mixed sorbents, *Adsorption*, 7(2001), 139-147.

29. A. Özcan, E. M. Öncü, A. S. Özcan, Kinetics, isotherm and thermodynamic studies of adsorption of Acid Blue 193 from aqueous solutions onto natural sepiolite, *Colloids Surf., A,* 277(2006), 90-97.

30. A. S. Özcan, A. Özcan, Adsorption of acid dyes from aqueous solutions onto acid-activated bentonite, *J. Colloid Interface Sci.*, 276(2004), 39-46.

31. N. M. Mahmoodi, B. Hayati, M. Arami, C. Lan, Adsorption of textile dyes on Pine Cone from colored wastewater: Kinetic, equilibrium and thermodynamic studies, *Desalination*, 268(2011), 117-125.